Indonesian Journal of Cancer Chemoprevention, June 2024
ISSN: 2088–0197
e-ISSN: 2355-8989

Analysis of SARS-CoV-2 spike-Induced Syncytia with Lifeact-GFP as Biosensor Using High-Content Screening Instrument for Automated Syncytia Counting

Dita Fauziah[1], Endah Puji Septisetyani[2]*, Eti Yerizel[1], Ria Fajarwati Kastian[2]

[1]Biomedical Science Study Program, Faculty of Medicine, Universitas Andalas
[2]Research Center for Genetic Engineering, National Research and Innovation Agency

Abstract

SARS-CoV-2 is believed to cause cytopathic effects in forming multinucleated cells, known as syncytia. Syncytia due to SARS-CoV-2 infection found in lung tissue samples of COVID-19 patients represents a case of COVID-19 with a poor prognosis. Therefore, it is very important to study the mechanism of syncytia formation and to test candidate materials that can inhibit the occurrence of syncytia and potentially be applied in the treatment or prevention of COVID-19. Since syncytia counting and analysis are time-consuming, we utilized a high-content screening (HCS) instrument in this study to automate syncytia analysis. We used 293T cells transfected with plasmids to express the SARS-CoV-2 spike, human angiotensin-converting enzyme-2 (hACE-2), and a plasmid encoding lifeact-GFP as an F-actin biosensor to facilitate syncytia analysis using the HCS instrument. In this study, syncytia analysis was carried out using HCS software. The HCS application categorizes cells as multi-nuclei by counting the number of cell nuclei stained with DAPI in cells that emitted green fluorescence due to lifeact-GFP expression. Syncytia analysis is time-consuming because of the calculation of the number of syncytia formed in a confluent cell monolayer culture. Hopefully, utilizing the HCS platform can accelerate the test of syncytia inhibition after various treatments using test compounds.

Keywords: *293T cells, high-content analysis, SARS-CoV-2, spike, syncytia.*

INTRODUCTION

SARS-CoV-2 is a pathogenic virus that caused the COVID-19 pandemic in 2019-2023. In infecting host cells, there are 2 pathways for SARS-CoV-2 to enter cells: endocytosis (endosomal entry) and cell fusion (cell surface entry). The main difference in these mechanisms lies in the type of protease involved. Although the types are different, these proteases have the same role, namely, to cut the part of the spike protein that has bound to hACE2 so that one part of the spike protein, namely the S2 domain, can mediate fusion between the viral membrane and the host cell membrane or host cell vesicle membrane (Fraser, *et al*., 2022; Padmanabhan, *et al*., 2020; Zhao, *et al*., 2021).

The endosomal mechanism pathway involved the activity of proteases, including cathepsin L/B (CTSL/CTSB). The mechanism

Submitted: October 15, 2024
Revised: December 19, 2024
Accepted: December 19, 2024
Published online: January 29, 2025

*Corresponding author: enda041@brin.go.id

in this pathway begins when the spike protein binds to the hACE2 receptor. The spike binding complex with the hACE2 receptor causes the host cell membrane to form a pocket immersed in the host cell cytoplasm. The deeper the pocket, the more viruses will be trapped in the pocket, which will form a vesicle. The vesicle that has been formed will induce protease to cleave the spike protein and cause partial fusion of the viral membrane with the membrane on the host cell vesicle. The genome of the SARS-CoV-2 virus exits the virus and enters the cell after the fusion occurs (Cesar-Silva, *et al*., 2022).

As for the mechanism of virus entry by cell fusion, the difference is that the protease involved is TMPRSS2, and in this mechanism, no vesicles are formed as in the endosomal virus entry mechanism (Wang, *et al*., 2023). Of the two mechanisms of virus entry, there are several differences in several variants of the SARS-CoV-2 virus that enter the host cell, which can affect the transmission level.

As recently reported for the SARS-CoV-2 Delta variant, the most dominant pathway for virus entry into cells is the TMPRSS2-dependent cell fusion pathway (Mlcochova, *et al*., 2021). In contrast to the Delta variant, the dominant pathway for the Omicron variant is the cathepsin-dependent endosomal pathway. The differences in virus entry pathways can affect the level of transmission. The endosomal pathway allows the virus to infect more cells even under low exposure conditions, so viruses that predominantly use this pathway are considered more infectious. However, syncytia formation in the endosomal pathway has been reported to be less than in the cell fusion pathway (Peacock, *et al*., 2022; Willett, *et al*., 2022).

SARS-CoV-2 is believed to cause cytopathic effects in forming multinucleated cells known as syncytia. Syncytia due to SARS-CoV-2 infection was first found in lung tissue samples of COVID-19 patients who had died. It was concluded that syncytia were found in COVID-19 cases with poor prognosis. Several variants of the SARS-CoV-2 virus can induce the formation of syncytia with different efficiencies. Virus variants that induce viral entry through a fusion mechanism, such as the Delta variant, can induce syncytia formation more efficiently than viruses that induce viral entry through an endosomal mechanism, such as the Omicron variant (Peacock, *et al*., 2022; Willett, *et al*., 2022). The induction of syncytia formation needs to be studied in vitro to study its formation mechanism and to test candidate inhibitors of syncytia formation.

In previous studies, microscopic observations were only carried out to obtain a qualitative analysis of syncytia formation. While more quantitative observations can be carried out using flow cytometry (Wünschmann and Stapleton, 2000) or reporter assays using luciferase (Zeng, *et al*., 2022). However, syncytia can also be counted manually based on the formation of multinucleated cells, but this is very time-consuming considering that one well of a multi-well plate consists of multiple microscope fields, and testing is usually carried out in more than one treated well (Septisetyani, *et al*., 2024). This study analyzed image-based syncytia by automated counting using a high-content screening (HCS) instrument.

MATERIALS AND METHODS

Cell Culture

The 293T cells (ECACC #12022001) are a collection of the Research Center for Genetic Engineering, National Research and Innovation Agency (BRIN), Cibinong, Indonesia. The cells were cultured in a high-glucose Dulbecco's modified Eagle's medium (DMEM) (Gibco, Invitrogen, Canada) containing 10% fetal bovine serum (FBS) and 1% antibiotics (100 µg/ml streptomycin and 100 IU/ml penicillin). The cells were maintained inside an incubator with 5% CO_2 at 37°C for optimal growth.

Indonesian Journal of Cancer Chemoprevention, June 2024
ISSN: 2088–0197
e-ISSN: 2355-8989

Expression Plasmids

The recombinant plasmids used in the study were pcDNA3.1-SARS2-Spike (Addgene plasmid #145032, gift from Fang Li) (Shang, *et al*., 2020) to express SARS-CoV-2 spike and pEGFP-C1 Lifeact-EGFP (Addgene #58470, http://n2t.net/addgene:58470, a gift from Dyche Mullins) (Belin, *et al*., 2015) to express a cytoplasmic actin filament reporter Lifeact. pcDNA3.1-hACE2 (a gift from Fang Li; Addgene plasmid #145033) (Shang, *et al*. 2020),TMPRSS2 (a gift from Roger Reeves; Addgene #53887) (Edie, *et al*., 2018).

Recombinant Plasmid Preparation

Recombinant *E. coli* harbouring expression plasmid was cultured in 5 mL Luria Bertani (LB) medium containing 50 mg/L ampicillin in an incubator at 37°C with 150-180 rpm shaking. Then, the culture was scaled up into 400 mL culture medium and incubated for about 16-18 h. At the end of incubation, the cell suspension was harvested by centrifugation. The recombinant plasmid was prepared from the cell pellet by a plasmid maxiprep kit (Qiagen) following the manufacturer's instructions, and the plasmid DNA concentration was determined using a microvolume spectrophotometer (Nanodrop, Thermo Fisher Scientific).

Transfection Condition

Confluent cell monolayers were transfected with recombinant plasmid DNA by cationic polymer-mediated transfection. We used transfection-grade linear polyethyleneimine (PEI) with a molecular weight of 40,000 (PEI Max, Polyscience) in a DNA-polymer ratio of 1 to 3. Each DNA and PEI was separately diluted with serum-free OptiMEM, then mixed and vortexed to produce nano-size particles. After about 15 minutes of incubation, the transfection mix was introduced into the cell culture and further incubated in the incubator overnight.

Immunofluorescence Staining (IF Staining)

Cells at a density of 160,000/mL were seeded onto a gelatine-coated coverslip within a 24-well cell culture plate. The cells were incubated for about 5-6 h, transfected with recombinant plasmid using PEI, and incubated overnight inside an incubator. The following day, the culture medium was refreshed, and cells continued to be incubated in the incubator for another 5-6 h. At the end of incubation, the cells were fixed with 4% paraformaldehyde (PFA) and proceeded for IF staining. Cells were permeabilized with 0.2% triton-X for 10 minutes, washed with PBS, and then incubated with 1% BSA as a blocking reagent. After about one hour of incubation, the cells were incubated with primary antibody (anti-spike-antibody (Abcam, Cambridge, United Kingdom), anti-hACE2 antibody (Sigma, St. Louis, Missouri, US)) with a dilution of 1:250 and kept overnight at 4°C. The next day, the cells were washed with PBS and then incubated for about 2 h with secondary antibodies that conjugated with a fluorochrome (Alexa Fluor 488 or Alexa Fluor 594) (Invitrogen) added with rhodamine-conjugated phalloidin (Abcam) for F-actin staining. After washing with PBS, the cells on the coverslip were mounted with a DAPI-containing mountant (Abcam) and fixed in a microscope slide.

Cell Imaging

Cell observation was performed using a motorized fluorescence microscope (Olympus IX83, Olympus, Japan) in a dark condition using a 60x lens and adding immersion oil. The images were captured using a CMOS camera (DP75, Olympus, Japan).

Automation of Syncytia Analysis by High-Content Screening (HCS)

Syncytia induction in HEK293T cells was performed according to a previously published

article (Septisetyani, *et al*., 2024). Cells with a density of 160,000 cells/ml were seeded into an optical 96-well plate of black polystyrene (Nunc 165305) 100 µl/well and incubated overnight. The next day, the cells were transfected with SARS-CoV-2 spike, hACE2, and lifeact-GFP expressing plasmids using PEI and incubated for about 4-5 h. Then, the medium was changed, and the cells were continued to be incubated overnight. At the end of incubation, the cells were stained for DAPI and proceeded to the HCS instrument. For HCS analysis, the colony formation assay analysis method was chosen to quantify the syncytia as fused cells. For channel 1, the DAPI indicator was selected for nuclei staining, and then for channel 2, the GFP indicator was selected to measure the signal of lifeact-GFP, which worked as a cell biosensor with corresponding excitation and emission wavelengths. Then, the setting for nuclei and fused cells was validated to obtain the correct measurement. The analysis of syncytia number was performed based on member ch2, which represented nuclei number inside syncytia, and the selected object, which represented syncytia where in each well of 96-well plate images of 9 microscope fields were taken.

RESULTS

Observation of Spike, hACE2, and TMPRSS2 Expression with IF Staining

The immunofluorescence (IF) staining technique is a technique used to detect the localization of target proteins in cells by detecting fluorescent signals derived from antigen-antibody reactions utilizing fluorescence-conjugated primary or secondary antibodies to tag the target proteins. The fluorescence signals can be visualized using a fluorescence microscope with a suitable filter to detect the fluorochrome used. This study used a secondary antibody conjugated with Alexa Fluor 488 as a fluorochrome that works as a green-fluorescent dye with a maximum excitation/emission wavelength at 499 nm and 520 nm (Thermo Fisher Scientific).

In Figure 1, column 1, the expression of the spike and hACE2 proteins can be seen. The expression level can be observed from the level of green fluorescence intensity and the extent of the area or part of the green cell. In Figure 1, the spike and hACE2 proteins can be detected in the cytoplasm and cell membrane. In cells expressing spike protein and hACE2, the

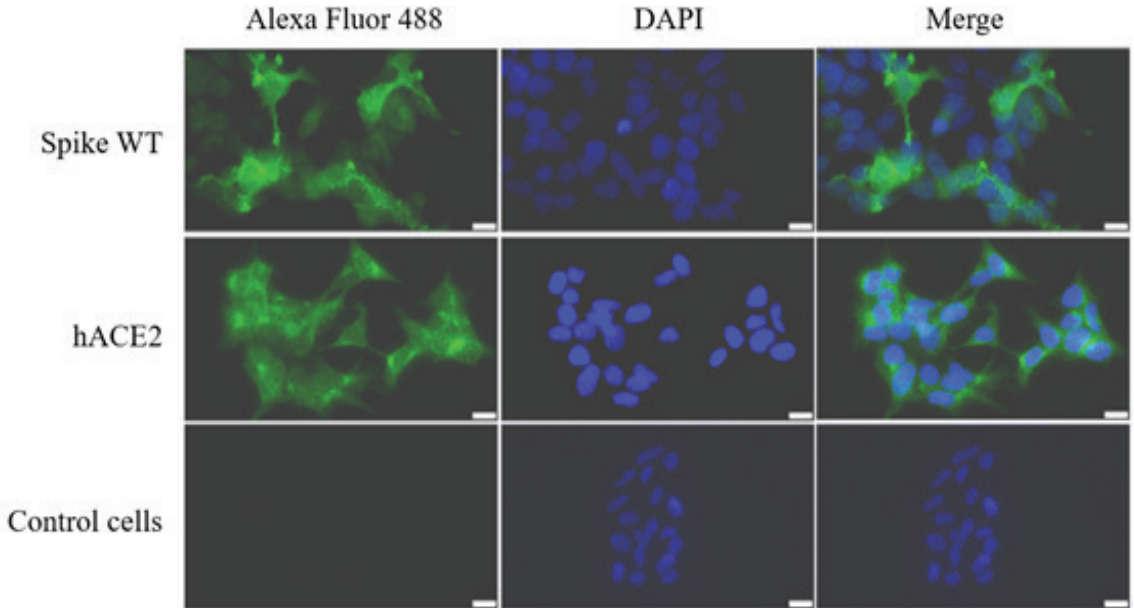

Figure 1. Detection of ectopic recombinant protein expression. Expression of SARS-CoV-2 spike and hACE2 in 293T cells was confirmed by immunofluorescence (IF) staining.

intensity of the green fluorescence is higher in the cell membrane compared to the cytoplasm. However, there is a slight difference in characteristics of cells expressing spike protein, namely the formation of filopodia. The presence of filopodia in cells expressing spike protein indicates that the cells are more active in moving so that it can make it easier to find their receptors, namely hACE2. In addition to using the Alexa 488 fluorescent dye, this IF staining technique is usually also equipped with nuclei staining, such as DAPI. Nuclei staining is mandatory because it is also used to distinguish cells or non-cells. In addition, DAPI dye also has the function of making it easier to count cells or distinguish cell types based on the number of nuclei.

Analysis of Syncytia Formation Using High- Content Screening (HCS)

Syncytia are multinucleate cells or cells with many nuclei. The morphology of syncytia can be observed in the image below (Figure 2A). When observed with a fluorescence microscope, the 293T cells observed as syncytia can be characterized by cells with more than one cell nucleus or multiple nuclei with GFP expression.

This study used the HCS instrument to assist in quantifying syncytia. The instrument analyzes syncytia based on GFP expression and the number of cell nuclei in the recombinant cells. Several categories used in this instrument include selected objects that appear as dotted blue lines that represent syncytia, rejected objects that appear

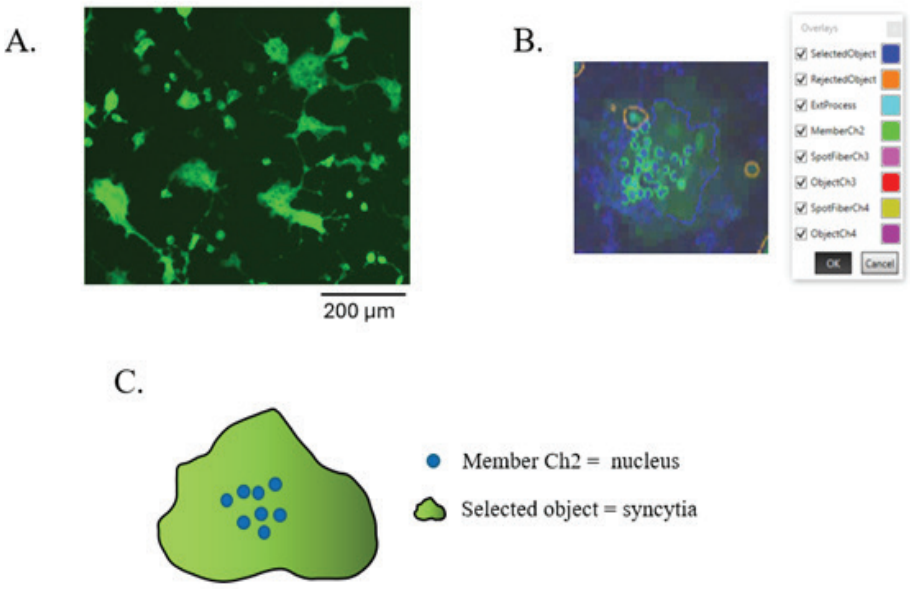

Figure 2. Observation of syncytia induced by spike, ACE2, and TMPRSS2 expression in 293T cells and channel categorization for analysis using HCS. A. Syncytia with lifeact-GFP as a biosensor. B. Segmentation of syncytia for automated counting using HCS software. B. Categorization of the HCS instrument as a basis for syncytia quantification. The instrument analyzes cells with green fluorescent and classifies them as syncytia if the number of cell nuclei in them is more than 1. Blue dashed line (selected object) = syncytia, green line (member Ch2) = cell nuclei located inside syncytia, orange line = GFP-expressing cells that are considered not as syncytia). C. Sketch of syncytia analysis segmentation using HCS.

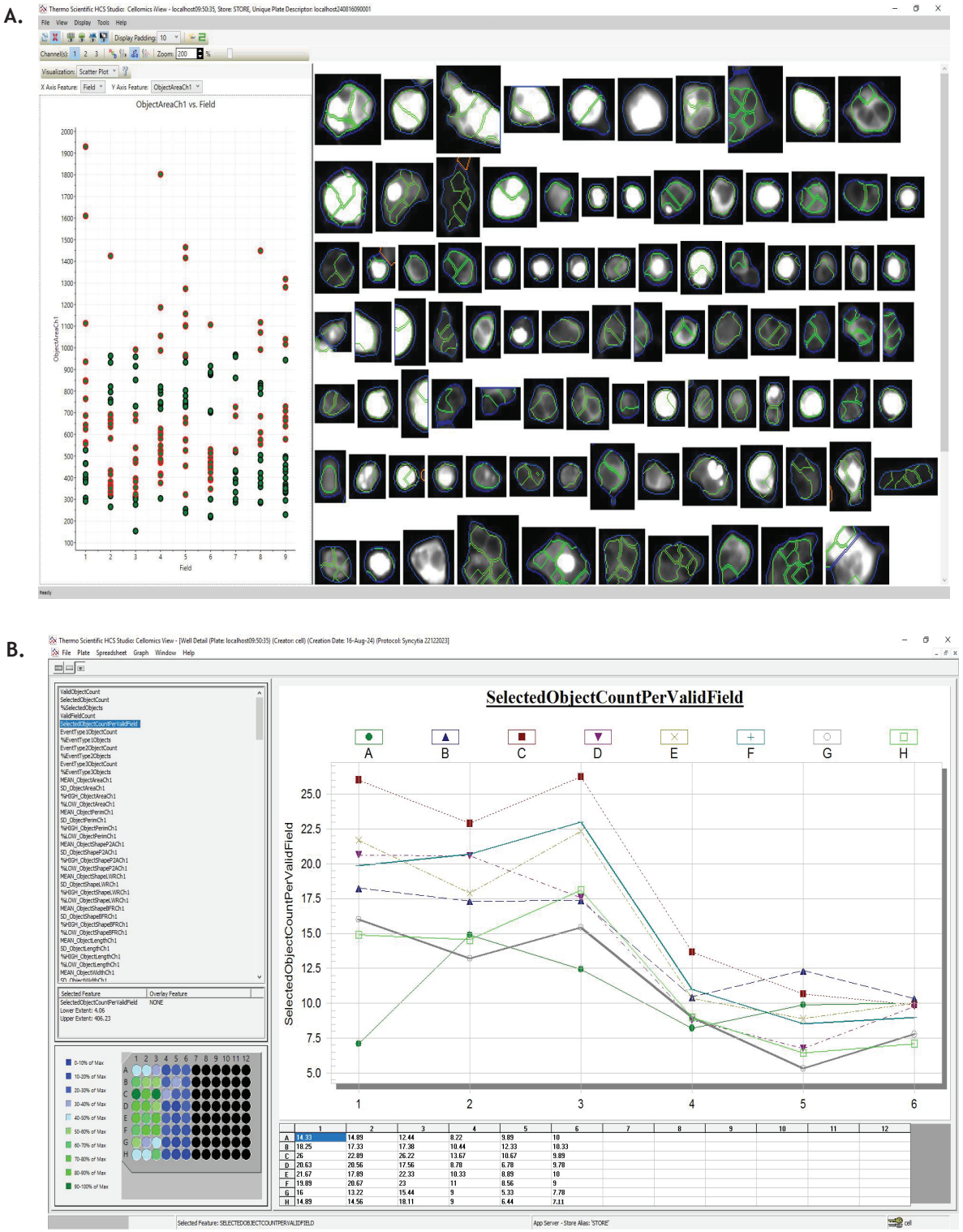

Figure 3. Representative image of results after analysis of syncytia using HCS for automation. A. Screenshot of an HCS software presentation after data acquisition and syncytia analysis of images taken from 9 different microscope fields from a well of 96-well plate. B. Screenshot of an HCS software showing the average syncytia number per well (selected object count per valid field).

as orange crisps that are cells expressing GFP that are not classified as syncytia, and MemberCh2 that appears as a green line and indicate cell nuclei (Figure 2B-C). During data acquisition, the instrument was set to acquire 9 photos from 9 different microscope fields for each well on a 96-well plate and calculate it as the average syncytia number. The general screenplays shown after a single HCS running are presented here (Figure 3). The result may be shown as a dot plot in the cell view. Each dot represented one syncytium of one microscope field in which once it is clicked, we can see the image of the syncytium selected. The 9 fields indicate each image taken per microscope field (Figure 3A). Moreover, the data can be viewed as a line curve to show our selected data. Here, we showed the selected object count per valid field representing each well's average syncytia number per valid field (Figure 3B).

DISCUSSION

HEK293T cells are a type of adherent cell that is widely used as a medium to produce recombinant proteins, virus-like particles, or viral vectors (Tan, *et al*., 2021). These cells are derived from human embryonic kidney cells transformed with adenovirus type 5 (Ad5) DNA fragments and formed by the expression of a temperature-sensitive polyomavirus simian virus 40 (SV40) mutant T antigen (DuBridge, *et al*., 1987; Graham, *et al*., 1977; Gupta, *et al*., 2020; Rio, *et al*., 1985). The presence of the SV40 mutant T antigen in HEK293T cells allows the inhibition of TP53 (tumor protein p53) expression which is required for efficient virus replication and cell transformation (Lilyestrom, *et al*., 2006). In making SARS CoV-2 model cells, HEK293T cells must be able to express one or several proteins that are part of the SARS CoV-2 genome or its receptor. One type of protein that is often used because it is often the target of COVID-19 treatment is the spike protein. The creation of SARS CoV-2 model cells is done by transfecting or inserting a plasmid containing the gene encoding the spike protein into HEK293T cells so that the surface of the cell membrane will express the spike protein. Often the creation of HEK293T cells that express the spike protein (HEK293T/Spike cells) is also accompanied by the creation of 293T cells that express its receptors, namely hACE2 and TMPRSS2 protease (293T/hACE2.TMPRSS2 cells) which are expressed on the surface of the human lung cell membrane. The aim is to study the mechanism of virus internalization into host cells and the formation of syncytia as well as the factors that influence the binding between spike and hACE2. TMPRSS2 which is often tested to find potential drugs to treat COVID-19 (Battles & McLellan, 2019; Buchrieser, *et al*., 2020).

Syncytia are multinucleated cells with larger than normal cell sizes (Buchrieser, *et al*., 2020). Under normal conditions, syncytia can be found in osteoclast cells in bones, hepatocyte cells in the liver, heart muscle cells, and myoblast cells in skeletal muscles (Bar-Shavit, 2007; Li, *et al*., 2020; Pajcini, *et al*., 2008; Shalakhmetova, *et al*., 2009). Clinically, in the lungs of patients infected with the SARS CoV-2 virus with severe conditions, a number of dysmorphic lung cells are found, which are often found as syncytia (Bussani, *et al*., 2020). Syncytia formation in the lung cells of COVID-19 patients indicates that the infection is already at an advanced stage. In *in vitro* studies, the mechanism of syncytia formation indicates intercellular transmission. Cells infected by the SARS-CoV-2 virus will synthesize spike protein as one of the units of the virus particle in the endoplasmic reticulum (ER) membrane and the golgi apparatus. The infected cells can express spike protein on the surface of their outer membrane, allegedly due to the replacement of the amino acid lysine with histidine and threonine at residues 1271 and 1273. The replacement of this amino acid causes the binding motif of cytoplasmic coat protein I (COPI) and COPII to the cytoplasmic tail of the spike protein to be less than optimal, so that the spike protein is susceptible to exiting the ER to the outer

membrane of the cell surface. As a result, the spike protein expressed on the membrane of infected cells allows it to bind to the hACE2 receptor on normal cells around it, forming syncytia (Cattin-Ortolá, *et al*., 2021).

The formation of syncytia in COVID-19 disease can have an impact on the pathological mechanisms caused. The pathological mechanisms caused start from the emergence of inflammatory responses, immune evasion mechanisms, and immune system elimination mechanisms (Zhang, *et al*., 2021), which cause an increase in the number of viruses. The inflammatory response is caused by apoptosis or death in syncytia which produces apoptosomal bodies. These apoptosomal bodies stimulate immune cells to provide an inflammatory response. Then in the apoptosis process, syncytia can produce viruses that can infect normal cells around them. Normal cells will be increasingly infected as syncytia formation increases (Singh, *et al*., 2015). Furthermore, when fusion occurs between syncytia and non-infected cells, the virus can avoid neutralizing antibodies by moving to the soon-to-be infected cells. The process of transmitting the virus to normal cells causes antibodies to be unable to recognize the viral antigen (Asarnow, *et al*., 2021; Cifuentes-Muñoz, *et al*., 2018).

HCS applies high-content analysis to determine the phenotype based on the captured images, where HCS can take multiple images of different microscope fields in each well. In a 96-well plate, the instrument can take 25 different microscope fields to cover almost the whole well area. For syncytia analysis, we used the colony formation assay analysis option available in the HCS software. On channel 1, the HCS instrument was set to measure DAPI as a marker for nuclei by selecting the appropriate excitation/emission filter for DAPI. On channel 2, the HCS instrument was set to measure the GFP signal from lifeact-GFP as an actin cytoskeleton marker that can represent the non-nuclei area. When HCS recognizes a GFP area containing more than one nucleus, it will be categorized as a syncytium. When validating the protocol, boundary settings must be made to exclude two or more adjacent GFP-positive cells that resemble syncytia. The bottleneck of the instrument in determining the target object lies in the channel and filter settings for data acquisition and validation of the procedure to obtain accurate data. Given that syncytia are giant cells with multiple nuclei, manual analysis of the number of syncytia formed in several microscope fields is not easy and time-consuming, especially when many treatments are performed. Therefore, a high-content screening (HCS) platform is very beneficial in accelerating syncytia analysis through automation.

CONCLUSION

The formation of syncytia is the result of the interaction of spike with its receptor, hACE2, which causes fusion between adjacent cells or is called cell-to-cell transmission. Cell-to-cell transmission is one way the virus infects indirectly. This syncytia inhibition test was conducted to find drug compounds that could potentially inhibit syncytia formation. By observing the syncytia formed, we can determine the effect of the drug compound from the number and size of the syncytia formed. The beginning of this test was the discovery of syncytia in human lung cells with chronic SARS CoV-2, so scientists made syncytia a biomarker or marker of the level of SARS CoV-2 infection. Hopefully, with this biomarker, drug compounds that can inhibit syncytia formation can be found.

ACKNOWLEDGMENTS

We thanked the Educational Fund Management Institution/National Research and Innovation Agency (LPDP/BRIN) (grant no. 102/FI/P-KCOVID-19.2B3/IX/2020 and

RIIM No. KEP-5/LPDP/LPDP.4/2022) and Research Organization for Life Sciences and Environment, BRIN (Research Program (DIPA Rumah Program) 2022) for financial supports. We were also grateful to the National Research and Innovation Agency for providing High Content Screening Platform CellInsight CX7 LZR Pro (Thermo Fisher Scientific), as well as Yinghua Qu, Ph.D. (Thermo Fisher Scientific), Ms. Irma Suryani Gultom (PT Nutrilab), and Ms. Arie Dwitrie (instrument operator, BRIN) for assistance during HCS operation.

REFERENCES

Asarnow, D., Wang, B., Lee, W., Hu, Y., Huang, C., Faust, B., *et al.*, 2021, Structural insight into SARS-CoV-2 neutralizing antibodies and modulation of syncytia, *Cell*, **184**(12), 3192-3204.e16.

Bar-Shavit, Z., 2007, The osteoclast: A multinucleated, hematopoietic-origin, bone- resorbing osteoimmune cell, *Journal of Cellular Biochemistry*, **102**(5), 1130–1139.

Battles, M.B., and McLellan, J.S., 2019, Respiratory syncytial virus entry and how to block it, *Nat Rev Microbiol.*, **17**(4), 233–245.

Belin, B.J., Goins, L.M., and Mullins, R.D., 2014, Comparative analysis of tools for live cell imaging of actin network architecture, *Bioarchitecture*, **4**(6), 189-202.

Buchrieser, J., Dufloo, J., Hubert, M., Monel, B., Planas, D., Rajah, M.M., *et al.*, 2020, Syncytia formation by SARS-CoV-2-infected cells, *The EMBO J.*, **39**(23), e106267.

Bussani, R., Schneider, E., Zentilin, L., Collesi, C., Ali, H., Braga, L., *et al.*, 2020, Persistence of viral RNA, pneumocyte syncytia and thrombosis are hallmarks of advanced COVID-19 pathology, *EBioMedicine*, 61.

Cattin-Ortolá, J., Welch, L.G., Maslen, S.L., Papa, G., James, L.C., and Munro, S., 2021, Sequences in the cytoplasmic tail of SARS-CoV-2 Spike facilitate expression at the cell surface and syncytia formation, *Nat Commun.*, **12**(1), 1–11.

Cesar-Silva, D., Pereira-Dutra, F.S., Moraes Giannini, A.L., Jacques, G., and de Almeida, C., 2022, The Endolysosomal System: The Acid Test for SARS-CoV-2, *Int J Mol Sci.*, **23**(9), 4576.

Cifuentes-Muñoz, N., Dutch, R.E., and Cattaneo, R., 2018, Direct cell-to-cell transmission of respiratory viruses: The fast lanes, *PLoS Pathog*, **14**(6).

DuBridge, R.B., Tang, P., Hsia, H.C., Leong, P.-M., Miller, J.H., and Calos, M.P., 1987, Analysis of Mutation in Human Cells by Using an Epstein-Barr Virus Shuttle System, *Mol Cell Biol.*, **7**(1) 379–387.

Edie, S., Zaghloul, N.A., Leitch, C.C., Klinedinst, D.K., Lebron, J., Thole, J.F., *et al.*, 2018, Survey of Human Chromosome 21 Gene Expression Effects on Early Development in Danio rerio, *G3 (Bethesda)*, **8**(7), 2215-2223.

Fraser, B.J., Beldar, S., Seitova, A., Hutchinson, A., Mannar, D., Li, Y., *et al.* 2022, Structure and activity of human TMPRSS2 protease implicated in SARS-CoV-2 activation, *Nat Chem Biol.*, **18**, 963–971.

Graham, F.L., Smiley, J., Russell, W.C., and Nairn, R., 1977, Characteristics of a human cell line transformed by DNA from human adenovirus type 5, *Journal of General Virology*, **36**(1), 59–72.

Gupta, A., Madhavan, M.V., Sehgal, K., Nair, N., Mahajan, S.,Sehrawat, T.S., *et al.*, 2020, Extrapulmonary manifestations of COVID-19, *Nat Med.*, **26**, 1017–1032.

Fraser, B.J., Beldar, S., Seitova, A., Hutchinson, A., Mannar, D., Li., Y., *et al.*, 2022, Structure and activity of human TMPRSS2 protease implicated in SARS-CoV-2 activation, *Nat Chem Biol.*, **18**, 963–971.

Li, W., Han, J.L., and Entcheva, E., 2020, Cardiac Excitation and Contraction: Syncytium cell growth increases Kir2.1 contribution in human iPSC-cardiomyocytes, *American Journal of Physiology - Heart and Circulatory*

Physiology, **319**(5), H1112.

Lilyestrom, W., Klein, M.G., Zhang, R., Joachimiak, A., and Chen, X.S., 2006, Crystal structure of SV40 large T-antigen bound to p53: interplay between a viral oncoprotein and a cellular tumor suppressor, *Genes & Development*, **20**(17), 2373–2382.

Mlcochova, P., Kemp, S.A., Dhar, M.S., Papa, G., Meng, B., Ferreira, I.A.T.M., *et al.*, 2021, SARS-CoV-2 B.1.617.2 Delta variant replication and immune evasion, Nature, **599**, 114–119.

Padmanabhan, P., Desikan, R., and Dixit, N.M., 2020, Targeting TMPRSS2 and Cathepsin B/L together may be synergistic against SARS-CoV-2 infection, *PLOS Computational Biology,* **16**(12), e1008461.

Pajcini, K.V., Pomerantz, J.H., Alkan, O., Doyonnas, R., and Blau, H.M., 2008, Myoblasts and macrophages share molecular components that contribute to cell-cell fusion, *J Cell Biol.*, **180**(5), 1005–1019.

Peacock, T.P., Brown, J.C., Zhou, J., Thakur, N., Sukhova, K., Newman, J., *et al.*, 2022, The altered entry pathway and antigenic distance of the SARS-CoV-2 Omicron variant map to separate domains of spike protein, *bioRxiv.*

Rio, D.C., Clark, S.G., and Tjian, R., 1985, A Mammalian Host-Vector System That Regulates Expression and Amplification of Transfected Genes by Temperature Induction, *Science*, **227**(4682), 23–28.

Septisetyani, E.P., Prasetyaningrum, P.W., Paramitasari, K.A., Suyoko, A., Himawan, A.L.I., Azzahra, S., *et al.*, 2024, Naringin Effect on SARS-CoV-2 Pseudovirus Entry and Spike Mediated Syncytia Formation in hACE2-overexpressing Cells, *HAYATI J Biosci.*, **31**(2), 336-347.

Shalakhmetova, T.M., Umbayev, B.A., Kolumbayeva, S.Z., and Kudryavtsev, B.N., 2009, About mechanisms of formation of multinuclear hepatocytes during toxic action of N-nitrosodimethylamine on rats, *Cell and Tissue Biology*, **3**(1), 61–70.

Shang, J., Ye, G., Shi, K., Wan, Y., Luo, C., Aihara, H., *et al.*, 2020, Structural basis of receptor recognition by SARS-CoV-2, *Nature*, **581**(7807), 221-224.

Singh, B.K., Hornick, A.L., Krishnamurthy, S., Locke, A.C., Mendoza, C.A., Mateo, M., *et al.*, 2015, The Nectin-4/Afadin Protein Complex and Intercellular Membrane Pores Contribute to Rapid Spread of Measles Virus in Primary Human Airway Epithelia, *J Virol.*, **89**(14).

Tan, E., Chin, C.S.H., Lim, Z.F.S., and Ng, S.K., 2021, HEK293 Cell Line as a Platform to Produce Recombinant Proteins and Viral Vectors, *Frontiers in Bioengineering and Biotechnology*, **9**.

Wang, H., Yang, Q., Liu, Q., Xu, Z., Shao, M., Li, D., *et al.*, 2023, Structure-based discovery of dual pathway inhibitors for SARS-CoV-2 entry, *Nat. Commun.* **14**, 7574

Willett, B.J., Grove, J., MacLean, O.A., Wilkie, C., Logan, N., De Lorenzo, G., *et al.*, 2022, The hyper-transmissible SARS-CoV-2 Omicron variant exhibits significant antigenic change, vaccine escape and a switch in cell entry mechanism, *MedRxiv.*, 2022.01.03.21268111.

Wünschmann, S. and Stapleton, J.T., 2000, Fluorescence-based quantitative methods for detecting human immunodeficiency virus type 1-induced syncytia, *J Clin Microbiol.*, **38**(8), 3055–3060.

Zeng, C., Evans, J.P., King, T., Zheng, Y., Oltz, E.M., Whelan, S.P.J., *et al.*, 2022, SARS-CoV-2 spreads through cell-to-cell transmission, *PNAS*, **119**(1), e2111400119.

Zhao, M.-M., Yang, W.-L., Yang, F.-Y., Zhang, L., Huang W-J., Hou, W., *et al.*, 2021, Cathepsin L plays a key role in SARS-CoV-2 infection in humans and humanized mice and is a promising target for new drug development, *Sig Transduct Target Ther.*, **6**, 134.

Zhang, Z., Zheng, Y., Niu, Z., Zhang, B., Wang, C., Yao, X., *et al.*, 2021, SARS-CoV-2 spike protein dictates syncytium-mediated lymphocyte elimination, *Cell Death Differ.*, **28**(9), 2765–2777.